•机械工程•

DOI:10.12454/j.jsuese.202400658

本刊网刊

SLM铺粉器结构对金刚石工具粉体铺展动力学机制的影响

黄国钦[1],张江涛[2,3*],祝小威[2],徐仰立[1],孙　龙[2],杜育隆[3],张云鹤[4]

(1.华侨大学 制造工程研究院,福建 厦门 361021;2.白鸽磨料磨具有限公司,河南 郑州 450199;
3.河南工业大学 机电工程学院,河南 郑州 450001;4.精工锐意科技(河南)有限公司,河南 郑州 450199)

摘　要:激光选区熔化(SLM)技术为结构功能一体化的金属基金刚石工具的制造提供了新方法。然而,粉床中金刚石颗粒分布不均匀以及堆积密度松散会导致金刚石工具性能变差。本文建立了金刚石/CuSn粉体铺展的离散元模型,探索线性、圆形和抛物线3种刮刀结构和滚筒铺粉器结构对铺粉质量和颗粒动力学行为的影响机制。结果表明,随着刮刀线性结构角度θ值和圆形结构系数c值的增加、抛物线结构系数p值的减小,以及滚筒直径d值的增加,铺粉器对颗粒斜向下的压力增大,导致颗粒的法向接触力增加,弱化铺粉器对颗粒的剪切作用,从而提高粉床质量。金刚石和CuSn颗粒的轨迹显示出相似的运动规律,但形状不规则的粗金刚石颗粒会形成强力链,引起颗粒堵塞,造成粉床中金刚石颗粒的体积分数先沿X方向呈现指数增加的趋势,之后在预定值附近波动,导致粉体铺展过程中金刚石颗粒的偏析。在本文给出的结构参数优化条件下,抛物线刮刀和滚筒铺粉器的铺粉质量相对较好,圆形刮刀次之,线性刮刀相对较差。研究结果对SLM制备金属基金刚石工具铺粉工艺的优化具有指导意义。

关键词:金属基金刚石;铺粉工艺;铺粉器结构;离散元模拟;激光选区熔化

中图分类号:TG48　　**文献标志码:**A　　**文章编号:**2096-3246(2026)06-0306-10

金刚石工具材料具有极高的硬度和耐磨性、较高的导热性能、较低的摩擦系数和热膨胀系数,性能优异,被广泛应用于冶金、建筑、精密制造等领域[1]。近年来,航空航天工业、电子通信和高端制造技术的发展,对航空航天用高性能钛合金、碳纤维复合材料、电子通信陶瓷、高端芯片等难加工材料的精密加工提出了严格的要求。金刚石工具朝着形状复杂化、结构精密化、性能高端化等方向发展,但烧结、钎焊、电镀等传统金刚石工具的制备方法受到其自身制备原理的限制,仅能实现规则结构的工具制备,复杂结构的金刚石工具的成形给生产加工的可行性、高效性、经济性带来了挑战[2]。

激光选区熔化(SLM)技术通过逐层铺粉、熔化的方式来直接制造零件,是目前增材制造领域最受关注的技术之一[3],该技术能实现空心、多孔、网格、异质材料和功能梯度等零件的制造,具有设计空间大、工序简单等特点[4],为实现金刚石工具的结构功能一体化制造提供了新方法,同时也是提高金刚石工具高精度、高效率、低热加工性能的重要手段。因此,采用SLM工艺来制备复杂结构的金刚石工具得到了工程界和学术界的广泛关注[5–6]。

SLM中金刚石工具的结构设计、热变形、残余应力和工艺建模等主题被研究较多[7]。其中,铺粉工艺是SLM技术的关键工序之一,对获得密实、平整均匀的粉床至关重要[8–9]。对铺粉工艺的研究表明,粉体铺展工艺过程对零件性能有重要影响。然而,实际的铺粉工艺过程会出现凹坑、划痕、粉床松散堆积、粉层分布不均匀、粉体偏析等问题,直接导致零件的性能较差甚至成形失败。因此,金刚石与金属基粉体的均匀铺粉是SLM制备金刚石工具的关键问题之一[10]。形状不规则的微米级金刚石粉体流动性难以保证,使其在金属粉体中均匀分布较为困难,易引发裂纹扩展、胎体对金刚石把持

收稿日期:2024 – 08 – 19　　**修回日期:**2024 – 11 – 27　　**网络出版日期:**2025 – 06 – 09

基金项目:国家重点研发计划项目(2021YFB3701800);国家自然科学基金项目(52105445);华侨大学制造工程研究院开放课题(2023IME–004);河南省高等学校重点科研项目(24A460006)

作者简介:黄国钦(1980—),男,教授. 研究方向:超硬磨料工具、高效精密加工. E-mail:smarthgq@hqu.edu.cn

* **通信作者:**张江涛,讲师, E-mail:zhangjiangtao@haut.edu.cn

力不足以及金刚石脱落等现象。

由于微米级粉体的流动形态难以量化描述，粉床质量的测量表征面临挑战；同时，微观的粉体流动难以捕捉。因此，实验研究的试错成本高，改善周期长。近年来，粉体铺展过程的离散元（DEM）模拟成为研究热点[11]。然而，铺粉工艺过程涉及粉体物性、铺粉器结构、铺粉工艺等众多参数[11−12]，铺粉工艺过程的颗粒动力学物理机制还没有被完全揭示。铺粉器的几何形状直接改变了铺粉器与颗粒的接触动力学行为，从而影响粉床质量。刮刀和滚筒是工业上使用最广泛的铺粉器[12]，Haeri[13]采用带有3个几何参数的超椭圆结构对刮刀的几何参数进行优化，优化后的刮刀结构可以获得与滚筒式铺粉相当的粉床质量，具有较好的实用性。Wang等[14]采用DEM研究了不同铺粉器结构对铺粉质量的影响，结果表明，与垂直刮刀相比，圆形和倾斜的刮刀结构可以形成更致密的粉层。粉层的不均匀性是由颗粒压缩回弹和颗粒堵塞现象造成的。滚筒式铺粉比垂直刮刀和倾斜刮刀更容易发生颗粒压缩回弹，导致粉层均匀性差。圆形刮刀系统受力最大，但由于没有颗粒的压缩回弹，铺粉质量更好。然而，现有的铺粉工艺研究大多是针对单一粉体材料的铺展过程，金属基金刚石复合粉体材料的铺粉工艺涉及非球形颗粒、多组分粉体颗粒动力学等复杂的科学工程问题，需要进一步的深入研究。

本文在前期研究[15]的基础上，选取线性、圆形和抛物线3种刮刀结构以及滚筒铺粉器结构，探索铺粉器结构对金属基金刚石复合粉体材料的铺粉质量和颗粒动力学行为的影响机制，优化铺粉工艺过程，可为SLM制备金刚石工具提供理论指导和技术支撑。

1　研究方法

1.1　离散元法

DEM通过求解牛顿第二定律方程来描述颗粒的运动。力−位移定律用于描述颗粒接触点处的相互作用。在颗粒接触或碰撞的情况下，使用迭代方法计算接触力并更新颗粒的位置。颗粒有两种运动方式，即平移运动和旋转运动，根据牛顿第二运动定律确定颗粒的运动方程[16]：

$$m_i\frac{\mathrm{d}v_i}{\mathrm{d}t}=\sum_{j=1}^{J}(F_{ij}^{\mathrm{n}}+F_{ij}^{\mathrm{t}})+F_i^{\mathrm{g}} \tag{1}$$

$$I_i\frac{\mathrm{d}\omega_i}{\mathrm{d}t}=\sum_{j=1}^{J}(T_{ij}^{\mathrm{t}}+T_{ij}^{\mathrm{r}}) \tag{2}$$

式(1)、(2)中，J为与颗粒i发生接触作用的所有颗粒总数，j为与颗粒i发生接触作用的颗粒索引，m_i、v_i、I_i和ω_i为颗粒i的质量、平移速度、惯性矩和角速度，F_{ij}^{n}、F_{ij}^{t}和F_i^{g}分别为法向力、切向力和重力，T_{ij}^{t}和T_{ij}^{r}分别为切向力和滚动摩擦力引起的力矩。

JKR（Johnson−Kendall−Roberts）模型[17]可以考虑颗粒之间的黏附力，已经被用来模拟增材制造铺粉工艺过程[18]。图1为颗粒法向接触力随法向重叠量变化的示意图，其中，$F_{ij,\mathrm{c}}^{\mathrm{n}}$为颗粒法向接触力，$\delta_{\mathrm{n}}$为法向重叠量。根据JKR理论[19]，当两个颗粒在A点碰撞接触时，由于范德华力的作用，法向接触力下降到某个值。颗粒的速度逐渐减小，变形也随之增大。当颗粒的动能转化为弹性能时，接触变形在D点处达到最大，且法向接触力也最大。此时，颗粒的加载过程结束，卸载过程开始。然后，法向重叠量在A点处返回0值，颗粒存储的动能被释放。然而，在这一点上，颗粒仍然被粘在一起。当颗粒继续分离时，黏附力将在C点处达到最大值，这一点上的力在JKR模型中被称为F_{pullout}。颗粒继续分离，直到S点颗粒完全分离。

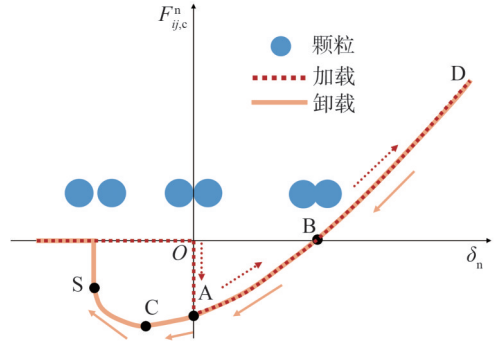


图1　颗粒法向接触力随法向重叠量变化的示意图

Fig. 1　Schematic diagram of the change of particles normal contact force with normal overlap

JKR模型考虑了范德华力对颗粒运动的影响，颗粒间法向接触力计算公式[20]为：

$$F_{ij,\mathrm{c}}^{\mathrm{n}}=\frac{4E^*}{3R^*}\alpha^3-4\sqrt{\pi\gamma E^*}\,\alpha^{\frac{3}{2}} \tag{3}$$

式中，R^*、E^*、γ和α分别为等效半径、等效杨氏模量、表面能和接触半径。

接触半径α和法向重叠量δ_{n}的关系为[21]：

$$\alpha^4-2R^*\delta_{\mathrm{n}}\alpha^2-\frac{4\pi\gamma}{E^*}R^{*2}\alpha+R^{*2}\delta_{\mathrm{n}}^2=0 \tag{4}$$

由式(3)、(4)可知，即使颗粒处于非接触状态，黏附力仍然存在。JKR模型提供了颗粒间非接触状态下黏附力的计算方法。颗粒之间的临界间隙$\delta_{\mathrm{n,c}}$和临界接触半径α_{c}分别通过式(5)、(6)计算[20]：

$$\delta_{\mathrm{n,c}}=\frac{\alpha_{\mathrm{c}}^2}{R^*}-\sqrt{\frac{4\pi\gamma\alpha_{\mathrm{c}}}{E^*}} \tag{5}$$

$$\alpha_{\mathrm{c}}=\frac{9\pi\gamma R^{*2}}{2E^*}\left(\frac{3}{4}-\frac{\sqrt{2}}{2}\right) \tag{6}$$

当颗粒之间的间隙大于临界间隙时，黏附力为0。

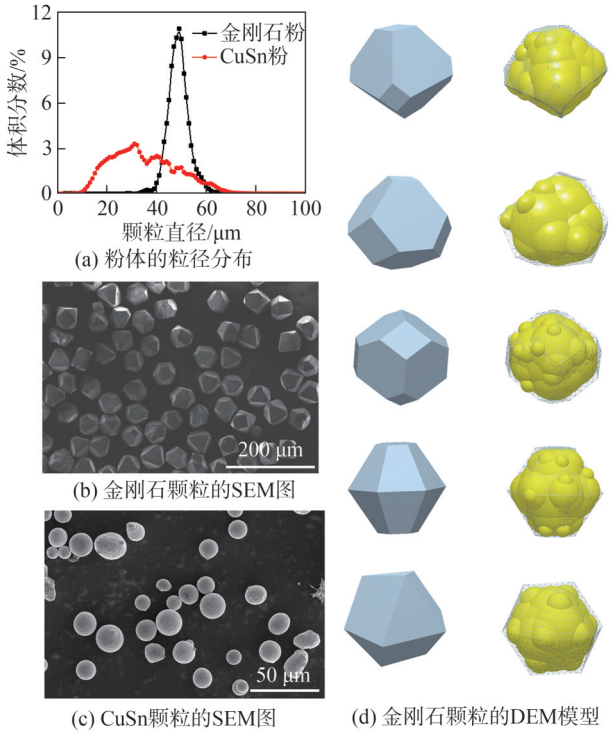
当颗粒未接触且间隙小于临界间隙时，JKR 模型提供了颗粒间黏附力最大值 F_{pullout}，其计算公式[21]为：

$$F_{\text{pullout}}=-\frac{3}{2}\pi\gamma R^{*} \tag{7}$$

关于 JKR 接触模型的信息详见文献[21–22]，为了简洁起见，本文不予赘述。

1.2 仿真条件

CuSn 材料是制备金属基金刚石工具时常用的金属结合剂，由于它的熔化温度低，可以避免金刚石颗粒的热损伤，非常适用于 SLM 加工工艺[23]。本文以金刚石和 CuSn 合金粉体为原料，采用扫描电子显微镜（SEM）观察颗粒的微观形貌。图 2 为粉体的粒径粒形特征[15]。如图 2 所示，CuSn 颗粒具有良好的球形度，在 DEM 模拟中，CuSn 颗粒的形状被简化为球体。对于金刚石非球形颗粒的几何模型，构造了 5 种典型的金刚石颗粒三维几何模型，并通过多球组合生成金刚石颗粒的 DEM 模型。在先前的研究工作[15]中，已经对两种粉体的粒径分布、形状特征、杨氏模量、表面能、恢复系数和摩擦系数等参数进行了表征，表 1 给出了 DEM 模拟所需的颗粒物理和接触特性参数[15]。



(a) 粉体的粒径分布　(b) 金刚石颗粒的SEM图　(c) CuSn颗粒的SEM图　(d) 金刚石颗粒的DEM模型

图 2 粉体的粒径粒形特征[15]

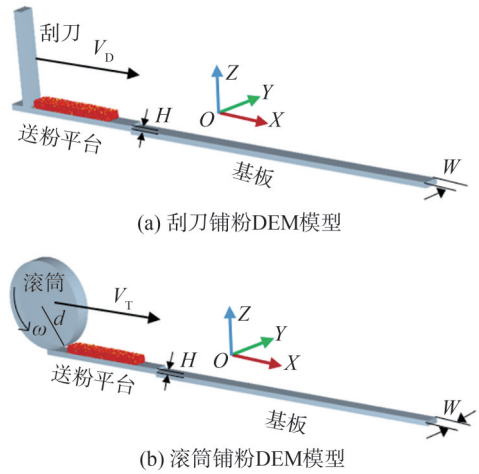
Fig. 2 Particle size and shape characteristics of powder[15]

在实际的铺粉过程中，成型区的尺寸和形状是多样的，本文将成型区简化为长方体（基板）。铺粉模拟系统由铺粉器（刮刀或滚筒）、送粉平台和基板组成，铺粉工艺的 DEM 模型如图 3 所示。基板的长度（X 方向）和宽度（Y 方向）分别为 15.0 mm 和 0.8 mm。

表 1 仿真中的 DEM 参数[15]

Tab. 1 DEM parameters in simulation[15]

材料属性	粉体	参数值
颗粒粒径 D_{50}/μm	CuSn 粉	32.7
	金刚石粉	48.2
材料密度 ρ/(kg·m^{-3})	CuSn 粉	8 730
	金刚石粉	3 563
弹性模量 E/GPa	CuSn 粉	120
	金刚石粉	1 141
泊松比 ξ	CuSn 粉	0.34
	金刚石粉	0.07
静摩擦系数 μ_s	CuSn 粉–CuSn 粉	0.60
	CuSn 粉–金刚石粉	0.61
	金刚石粉–金刚石粉	0.65
滚动摩擦系数 μ_r	CuSn 粉–CuSn 粉	0.08
	CuSn 粉–金刚石粉	0.07
	金刚石粉–金刚石粉	0.06
恢复系数 e	CuSn 粉–CuSn 粉	0.60
	CuSn 粉–金刚石粉	0.65
	金刚石粉–金刚石粉	0.80
表面能 γ/(mJ·m^{-2})	CuSn 粉–CuSn 粉	0.60
	CuSn 粉–金刚石粉	0.70
	金刚石粉–金刚石粉	0.80



(a) 刮刀铺粉DEM模型

(b) 滚筒铺粉DEM模型

图 3 铺粉工艺的 DEM 模型

Fig. 3 DEM of powder spreading processes

设置金刚石颗粒的体积分数为 15%，随机产生金刚石（黄色标记）和 CuSn 颗粒（红色标记），颗粒在重力的作用下沉积在送粉平台上。在实际的铺粉工艺过程中，颗粒主要沿着铺粉方向流动，颗粒的侧向流动对结果的影响很小[24–25]。因此，为了减少计算量，在侧向方向（Y 方向）的两侧设置周期性边界条件。在刮刀铺粉过程中，刮刀以恒定的速度沿 X 轴的正方向移动。图 3（a）中，V_D 为刮刀的平移速度，H 为铺粉层厚度，W 为基板宽度。在滚筒铺粉过程中，滚筒以恒定的速度

沿X轴的正方向平移并逆时针旋转。图3(b)中，V_T为滚筒的平移速度，ω为滚筒的旋转速度，d为滚筒的直径。铺粉工艺过程的模拟条件如表2所示。

表2　铺粉工艺过程的模拟条件

Tab. 2　Simulation conditions of spreading processes

参数	取值
铺粉器平移速度 V/(mm·s^{-1})	100
铺粉层厚 H/μm	150
滚筒转速 ω/(r·min^{-1})	100
刮刀线性结构角度 θ/(°)	0、60、90、120、150
刮刀圆形结构系数 c/mm	0.25、0.50、0.75、1.00、1.25
刮刀抛物线结构系数 p	0.1、0.5、1.0、1.5、2.0
滚筒直径 d/mm	2.5、5.0、7.5、10.0、12.5
基板长度 L/mm	15
基板宽度 W/mm	0.8
粉层采样区的长度 L_s/mm	10
粉层采样区的宽度 W_s/mm	0.8

针对刮刀结构，本文选取线性、圆形和抛物线3种典型的结构，通过参数化方程来改变刮刀的几何形状。

线性刮刀结构的方程为：

$$z_\theta = x/\tan\frac{\theta}{2} \tag{8}$$

圆形刮刀结构的方程为：

$$z_c = \sqrt{c^2 - x^2} + c \tag{9}$$

抛物线刮刀结构的方程为：

$$z_p = px^2 \tag{10}$$

式(8)～(10)中，z_θ为线性刮刀轮廓在竖直方向的坐标，z_c为圆形刮刀轮廓在竖直方向上的坐标，z_p为抛物线刮刀轮廓在竖直方向上的坐标，x为刮刀轮廓任意位置的水平坐标，θ为线性刮刀结构的角度，c为圆形刮刀的结构系数，p为抛物线刮刀的结构系数。刮刀的结构示意图如图4所示。

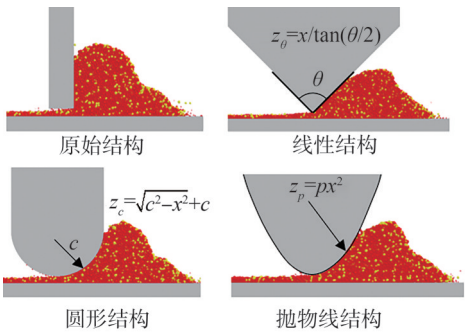


图4　刮刀结构的示意图

Fig. 4　Schematic diagram of blade structures

2　铺粉器结构对铺粉质量的影响

密实的粉层有助于提高粉体对激光能量的吸收并得到致密的零件。因此，粉层密度是评价粉床质量的重要指标。采用粉层的相对堆积密度表征粉层密实性，计算公式为：

$$\varphi = \frac{\sum_{i=1}^{N}\frac{4}{3}\pi R_i^3}{L_s W_s H} \tag{11}$$

式中，R_i为颗粒i的半径，N为铺粉完成后粉层中颗粒的总数量，L_s和W_s为基板上粉层采样区的长度(10 mm)和宽度(0.8 mm)。

SLM铺粉工艺中，金刚石颗粒随机分布在粉床中，存在颗粒偏析现象，会对金刚石工具的性能产生重要影响。在金刚石颗粒聚集的区域，参与加工的金刚石颗粒浓度较高，磨削力较弱，容易堵塞，降低磨削效率。而在金刚石颗粒较少的区域，参与加工的金刚石颗粒浓度较低，过大的冲击力会导致金刚石断裂与脱落[26–27]。为了表征金刚石颗粒在粉床中的均匀分布情况，将粉床划分成50个单元，每个单元的长度和宽度均为0.4 mm，单元的高度与粉层厚度相同。单元k中金刚石颗粒的体积分数V_k通过以下公式计算：

$$V_k = \frac{V_c}{V_c + V_{Cu}} \tag{12}$$

式中，V_c和V_{Cu}分别为单元k中金刚石和CuSn颗粒的体积。

粉床中金刚石颗粒的平均体积分数$\overline{V}_k$为：

$$\overline{V}_k = \frac{1}{n}\sum_{k=1}^{n} V_k \tag{13}$$

式中，n为粉床划分成单元的总数量。

金刚石颗粒体积分数的标准偏差S用于表征金刚石颗粒在粉床中的均匀分布，其定义为：

$$S = \sqrt{\frac{1}{n-1}\sum_{k=1}^{n}(V_k - \overline{V}_k)^2} \tag{14}$$

通常，相对堆积密度越大，S值越小，意味着粉层越密实，金刚石颗粒的分布也更加均匀。

图5为不同铺粉器结构对铺粉质量的影响。线性刮刀结构对铺粉质量的影响如图5(a)所示，需要说明的是，将刮刀原始结构(角度θ为0°)作为对比项，当角度θ从0°增加到90°，铺粉质量微量变化，随着角度θ从90°增加到150°，铺粉质量显著提高。圆形结构对铺粉质量的影响如图5(b)所示，随着圆形刮刀结构系数c从0.25 mm增加到1.25 mm，铺粉质量显著提高。抛物线结构对铺粉质量的影响如图5(c)所示，当结构系数p值从0.1增大到2.0时，相对堆积密度从0.36下降到0.29，标准偏差从0.031增加到0.041。滚筒直径对铺粉质量的影响如图5(d)所示，增加滚筒直径可以改善粉床质量。

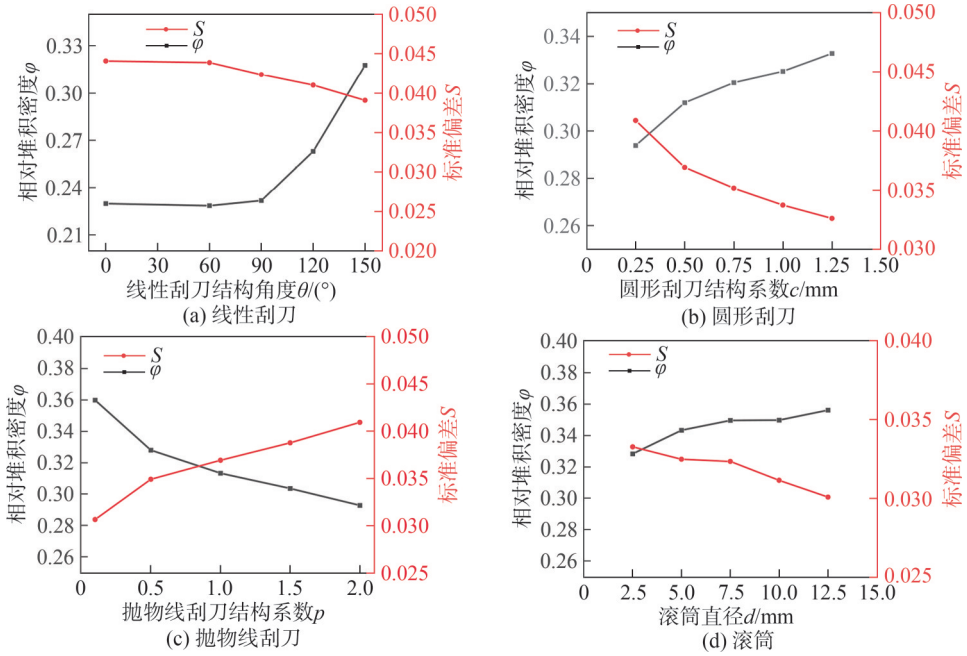


图5 铺粉器结构对铺粉质量的影响

Fig. 5 Effect of spreader structures on the powder spreading quality

图5的结果表明，刮刀原始结构的铺粉质量最差，改变刮刀的几何结构可以显著提高铺粉质量。在本文给出的结构参数优化条件下，综合对比铺粉器结构对铺粉质量的影响可知，抛物线刮刀和滚筒铺粉器的铺粉质量相对较好，圆形刮刀次之，线性刮刀相对较差。

3 颗粒动力学行为

3.1 颗粒流动行为

选用4组不同的铺粉器结构，详细阐明粉体铺展过程中的颗粒流动行为。在X轴方向上，将铺粉器前端的粉堆划分为6组，分别标记为红(X=2.0 mm)、绿(X=2.5 mm)、蓝(X=3.0 mm)、粉(X=3.5 mm)、黄(X=4.0 mm)和黑色(X=4.5 mm)，不同时刻的粉体流动形态如图6所示。随着铺粉器的平移运动，粉堆上部分颗粒受到剪切作用，在铺粉器的作用下向前运动，粉堆下部分通过铺粉器和基板之间间隙的颗粒类似于锥形料斗中孔口的颗粒流动[28]。此外，由于滚筒的复杂运动，在滚筒式铺粉过程中，颗粒在粉堆内部发生复杂的扩散和循环运动。而在刮刀式铺粉过程中，颗粒在粉堆内部的扩散运动相对较弱[12]，刮刀结构的改变对颗粒流动形态影响较小。

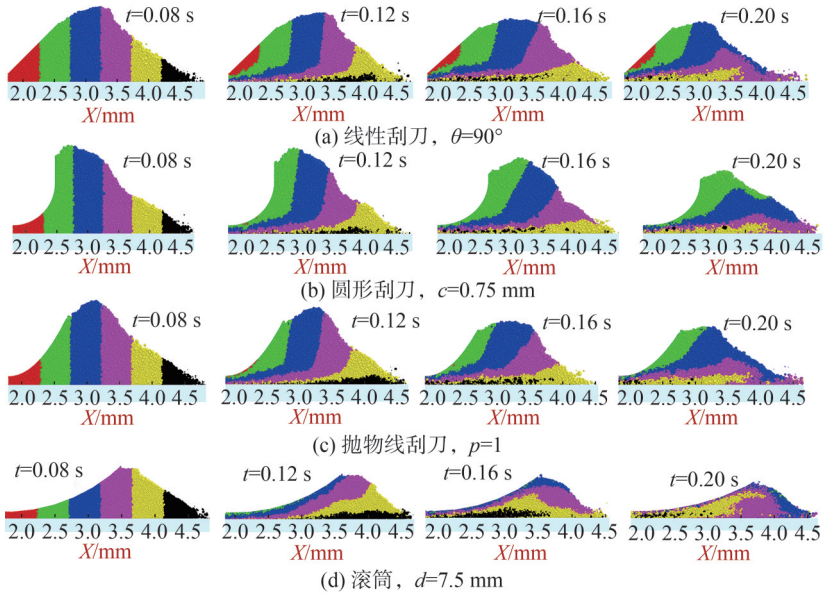
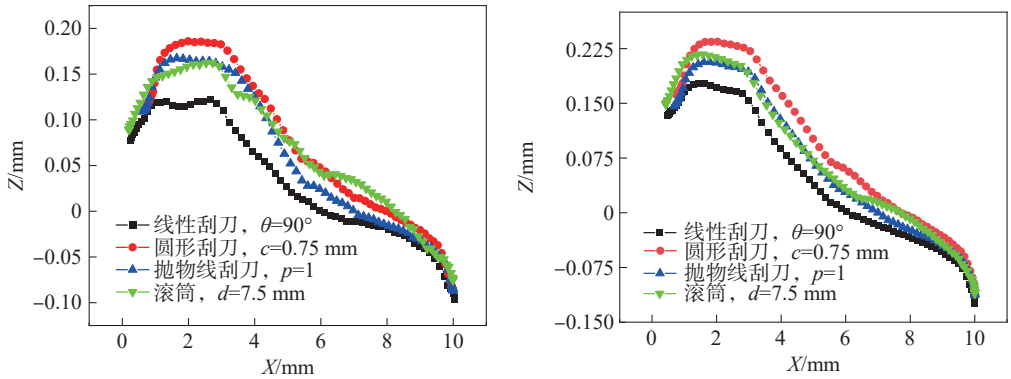


图6 不同时刻的粉体流动形态

Fig. 6 Powder flow patterns under different times

为了描述颗粒的运动轨迹，选取沉积在粉床中的金刚石和CuSn颗粒，追踪颗粒的X和Z坐标值，并求其平均值，颗粒的运动轨迹如图7所示。由图7可知，铺粉器结构会对颗粒的运动轨迹产生微弱的影响。但是，金刚石和CuSn颗粒的轨迹显示出相似的运动规律。在铺粉器的推动下，颗粒水平移动并上升，在高处波动一段距离。然后，由于重力的作用，颗粒沿着粉堆的斜坡雪崩而下。最后，颗粒通过铺粉器和基板之间的间隙沉积在基板上。



(a) 金刚石颗粒　　(b) CuSn颗粒

图7　颗粒的运动轨迹

Fig. 7　Trajectories of particles

3.2　颗粒的接触力链

当刮刀为原始结构时，接近基板处的粉体颗粒间的接触力链网络会变得疏松，但是会形成强力拱[29–30]，造成颗粒堵塞，这主要是刮刀对颗粒的剪切作用导致颗粒、基板与刮刀之间形成的强力链网络，改变刮刀几何机构的同时也改变了颗粒的接触行为。图8、9分别为不同铺粉器结构下的颗粒法向接触力图、接触力平均值。由图8、9可知，随着θ值、c值的增加和p值的减小，刮刀

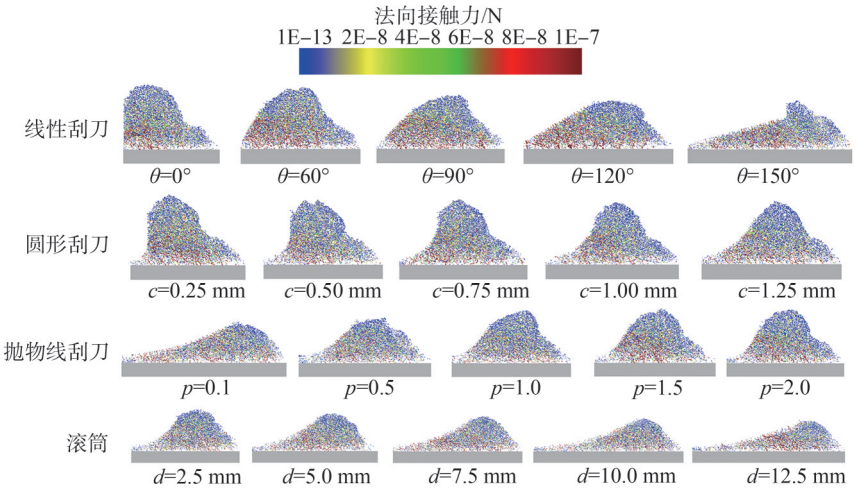


图8　不同铺粉器结构下的颗粒法向接触力

Fig. 8　Normal particle contact force diagrams under different powdering device configuration

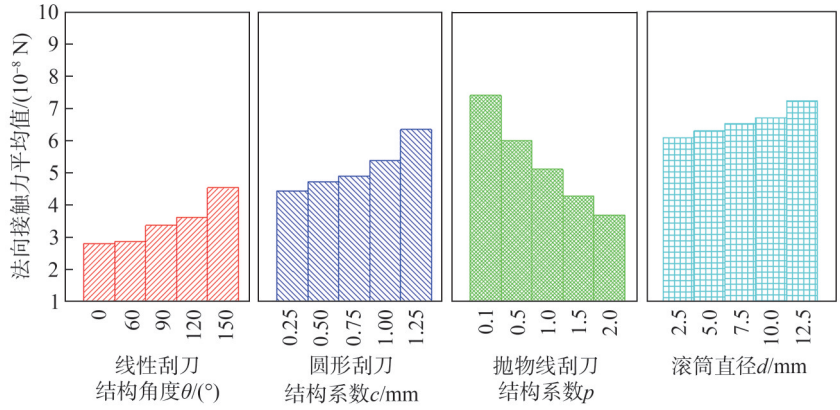


图9　不同铺粉器结构下的颗粒法向接触力平均值

Fig. 9　Average normal particle contact force under different powdering device configurations

会对颗粒形成斜向下的压力，导致颗粒的法向接触力增加，从而弱化刮刀对颗粒的剪切作用，提高粉床质量。对于滚筒铺粉器，增大滚筒直径会增加滚筒与粉堆相互作用的面积[31−32]，导致颗粒的法向接触力增加，并强化滚筒的压实作用，提高粉床质量。

3.3 金刚石颗粒体积分数的空间分布

将粉床在X方向上划分成25个单元，分析金刚石体积分数的空间分布规律。需要说明的是，由于铺粉DEM模型在Y方向设置了周期性边界条件，本文没有考虑金刚石体积分数在Y方向上的分布。图10为铺粉器结构对X方向上金刚石颗粒体积分数的影响。由图10可知，铺粉器结构对X方向上金刚石颗粒体积分数的影响无显著差异，但是金刚石颗粒的体积分数先沿X方向呈指数级增加的趋势，之后在预定值附近波动。这意味着粉床前端附近的金刚石颗粒浓度较低，导致粉体铺展过程中的颗粒偏析。主要原因是形状不规则的粗金刚石颗粒会形成强力链，导致颗粒堵塞，

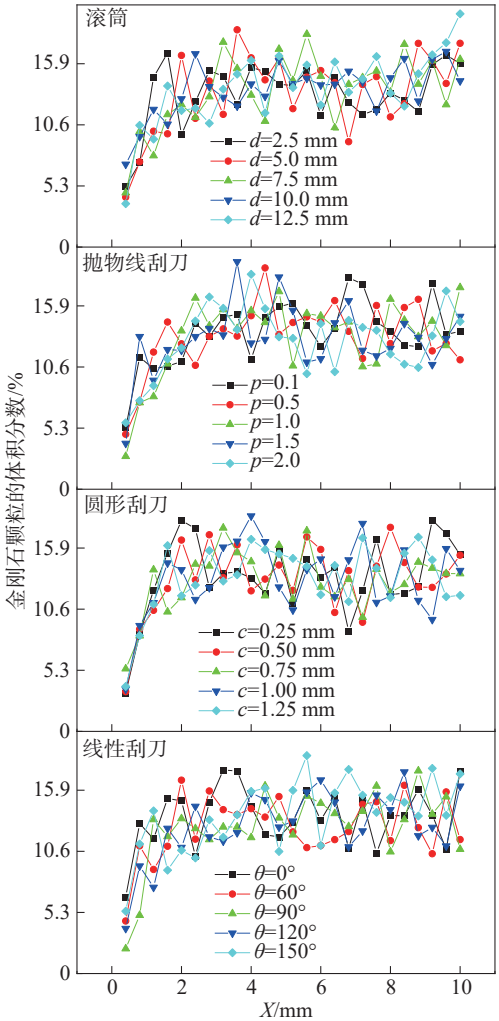


图10 铺粉器结构对X方向上金刚石颗粒体积分数的影响

Fig. 10 Effect of spreader structures on the volume fraction of diamond particles in the X direction

而细CuSn颗粒更容易穿过铺粉器和基板之间的间隙沉积在粉床的前端。因此，采用SLM技术制备金刚石工具时，建议避开粉床的前端，以提高金刚石工具性能的一致性和稳定性。

4 结 论

本文建立了金刚石/CuSn粉体铺展的离散元模型，探索线性、圆形和抛物线3种刮刀结构以及滚筒铺粉器结构对铺粉质量和颗粒动力学行为的影响机制。研究结论如下：

1）刮刀线性结构角度θ值和圆形结构系数c值的增加、抛物线结构系数p值的减小，以及滚筒直径d的增加，会增大铺粉器对颗粒斜向下的压力，导致颗粒的法向接触力增加，弱化铺粉器对颗粒的剪切作用，从而提高粉床质量。

2）在本文给出的结构参数优化条件下，综合对比铺粉器结构对铺粉质量的影响可得：抛物线刮刀和滚筒铺粉器的铺粉质量相对较好，圆形刮刀次之，线性刮刀相对较差。

3）粉床中金刚石颗粒的体积分数先沿X方向呈现指数级增加的趋势，之后在预定值附近波动，导致粉体铺展过程中金刚石颗粒的偏析。

参考文献：

[1] Zhang Liang. Filler metals, brazing processing and reliability for diamond tools brazing: A review[J]. Journal of Manufacturing Processes, 2021, 66: 651–668.

[2] Qin Jian, Yang Jiao, Long Weimin, et al. Research progress of additive technology of diamond and its composite materials[J]. Transactions of the China Welding Institution, 2022, 43(8): 102–112. [秦建, 杨骄, 龙伟民, 等. 金刚石及其复合材料增材技术研究进展[J]. 焊接学报, 2022, 43(8): 102–112.]

[3] Xiang Zhaowei, Yin Ming, Yin Guofu, et al. Influence of critical process parameters on the thermal physical process in selective laser melting[J]. Advanced Engineering Sciences, 2020, 52(1): 134–142. [向召伟, 殷鸣, 殷国富, 等. 激光选区熔化关键工艺参数对热物理过程的影响[J]. 工程科学与技术, 2020, 52(1): 134–142.

[4] Lu Bingheng. Additive mmanufacturing—current situation and future[J]. China Mechanical Engineering, 2020, 31(1): 19–23. [卢秉恒. 增材制造技术——现状与未来[J]. 中国机械工程, 2020, 31(1): 19–23.]

[5] Tian Chenchen, Wan Yi, Li Xuekun, et al. Study on the additively manufactured porous metal-bonded grinding wheel designed by octahedron lattice structure[J]. The International Journal of Advanced Manufacturing Technology,

2023,125(3):1743–1756.

[6] Li Xuekun,Wang Chao,Tian Chenchen,et al.Digital design and performance evaluation of porous metal-bonded grinding wheels based on minimal surface and 3D printing [J].Materials & Design,2021,203:109556.

[7] Li Shuai. Research on design, additive manufacturing and grrinding performance of structured grinding wheel[D]. Harbin: Harbin Institute of Technology,2022.[李帅.结构化砂轮的设计与增材成型及其磨削性能研究[D].哈尔滨:哈尔滨工业大学,2022.]

[8] Zhang Jiangtao, Tan Yuanqiang, Ji Caiyuan, et al. Research on the effects of roller-spreading parameters for nylon powder spreadability in additive manufacturing[J]. Chinese Journal of Theoretical and Applied Mechanics, 2021, 53(9):2416–2426.[张江涛,谭援强,纪财源,等.增材制造中滚筒铺粉工艺参数对尼龙粉体铺展性的影响研究[J].力学学报,2021,53(9):2416–2426.]

[9] Zhang Jiangtao, Tan Yuanqiang, Bao Tao, et al. Discrete element simulation for effects of roller's vibrations on powder spreading quality[J]. China Mechanical Engineering, 2020,31(14):1717–1723.[张江涛,谭援强,包涛,等.滚筒振动对铺粉质量影响的离散元模拟[J].中国机械工程,2020,31(14):1717–1723.]

[10] Tao Yakun,Gan Jie,Zhou Yan,et al.Research status and prospect of additive manufacturing diamond tools[J].Diamond & Abrasives Engineering,2022,42(5):511–517.[陶亚坤,甘杰,周燕,等.增材制造金刚石工具研究现状及展望[J].金刚石与磨料磨具工程,2022,42(5):511–517.]

[11] Zhang Jiangtao,Wang Ningchang,Chen Xing,et al.Particle gradations optimization for powder spreading in additive manufacturing[J].Materials & Design,2023,236:112509.

[12] Zhang Jiangtao, Tan Yuanqiang, Xiao Xiangwu, et al. Comparison of roller-spreading and blade-spreading processes in powder-bed additive manufacturing by DEM simulations[J].Particuology,2022,66:48–58.

[13] Haeri S. Optimisation of blade type spreaders for powder bed preparation in Additive Manufacturing using DEM simulations[J].Powder Technology,2017,321:94–104.

[14] Wang Lin,Yu Aibing,Li Erlei,et al.Effects of spreader geometry on powder spreading process in powder bed additive manufacturing[J].Powder Technology,2021,384:211–222.

[15] Zhang Jiangtao, Huang Guoqin, Xu Yangli, et al. Dynamic simulation of powder spreading processes toward the fabrication of metal-matrix diamond composites in selective laser melting[J].International Journal of Refractory Metals and Hard Materials,2024,118:106500.

[16] Cundall P A, Strack O D L. Discussion: A discrete numerical model for granular assemblies[J]. Géotechnique,1980, 30(3):331–336.

[17] Johnson K L, Kendall K, Roberts A D. Surface energy and the contact of elastic solids[J]. Proceedings of the Royal Society of London A Mathematical and Physical Sciences, 1971,324(1558):301–313.

[18] Li Wen, Liu Qipeng, Gao Yuehua, et al. Investigation into slm blade inclination effect on powder spreading behavior based on discrete element method[J]. Chinese Journal of Theoretical and Applied Mechanics,2024,56(3):774–784.[李雯,刘其鹏,高月华,等.基于离散元法的SLM刮刀倾角对粉末铺展行为的影响研究[J].力学学报,2024,56(3):774–784.]

[19] Chen Xizhong, Elliott J A. On the scaling law of JKR contact model for coarse-grained cohesive particles[J].Chemical Engineering Science,2020,227:115906.

[20] Hærvig J, Kleinhans U, Wieland C, et al. On the adhesive JKR contact and rolling models for reduced particle stiffness discrete element simulations[J]. Powder Technology, 2017,319:472–482.

[21] Chen Hui,Wei Qingsong,Wen Shifeng,et al.Flow behavior of powder particles in layering process of selective laser melting: Numerical modeling and experimental verification based on discrete element method[J]. International Journal of Machine Tools and Manufacture,2017,123:146–159.

[22] Yao Dengzhi, An Xizhong, Fu Haitao, et al. Dynamic investigation on the powder spreading during selective laser melting additive manufacturing[J]. Additive Manufacturing, 2021, 37:101707.

[23] Mao Yamei, Hei Hongjun, Gao Jie, et al. Research progress of brazing diamond and application of tools[J]. Journal of Mechanical Engineering,2022,58(4):80–93.[毛雅梅,黑鸿君,高洁,等.钎焊金刚石研究进展及其工具的应用[J].机械工程学报,2022,58(4):80–93.]

[24] Wu Qiong,Qiao Chuang,Wang Ju,et al.Adaptability investigations on bottom modified blade in powder spreading process of additive manufacturing[J]. Additive Manufacturing,2022,49:102477.

[25] He Yi, Hassanpour A, Bayly A E. Combined effect of particle size and surface cohesiveness on powder spreadability for additive manufacturing[J].Powder Technology,2021,392: 191–203.

[26] Yang Zhibo, Zhang Mingjun, Zhang Zhen, et al. A study on diamond grinding wheels with regular grain distribution using additive manufacturing (AM) technology[J]. Materials & Design,2016,104:292–297.

[27] Xiao Xiangwu,Jin Yufeng,Peng Ruitao,et al.Microscale viscous sintering model application to the preparation of metal bonded diamond grinding wheels[J]. International Journal of Refractory Metals and Hard Materials,2023,114:106242.

[28] Fouda Y M,Bayly A E.A DEM study of powder spreading in additive layer manufacturing[J]. Granular Matter, 2019, 22(1):10.

[29] Xu Rui,Nan Wenguang. Analysis of the metrics and mechanism of powder spreadability in powder-based additive manufacturing[J].Additive Manufacturing,2023,71:103596.

[30] Nan Wenguang, Pasha M, Bonakdar T, et al. Jamming during particle spreading in additive manufacturing[J]. Powder Technology,2018,338:253–262.

[31] Zhang Jiangtao,Tan Yuanqiang,Bao Tao,et al.Discrete element simulation of the effect of roller-spreading parameters on powder-bed density in additive manufacturing[J]. Materials,2020,13(10):2285.

[32] Sehhat M H, Mahdianikhotbesara A.Powder spreading in laser-powder bed fusion process[J]. Granular Matter, 2021, 23(4):89.

Effect of SLM Spreader Structures on the Powder Spreading Dynamics Mechanism of Diamond Tools

HUANG Guoqin[1], *ZHANG Jiangtao*[2,3*], *ZHU Xiaowei*[2], *XU Yangli*[1], *SUN Long*[2], *DU Yulong*[3], *ZHANG Yunhe*[4]

(1.Institute of Manufacturing Engineering, Huaqiao University, Xiamen 361021, China;
2.White Pigeon Abrasive Tools Co., Ltd., Zhengzhou 450199, China;
3.School of Mechanical and Electrical Engineering, Henan University of Technology, Zhengzhou 450001, China;
4.Precision Industry Revolution Equipment Technology (Henan) Co., Ltd., Zhengzhou 450199, China)

Abstract:

Objective Selective laser melting (SLM) technology provides a new approach to the integrated manufacturing of metal-matrix diamond tools with integrated structural and functional features, attracting considerable interest from academic and technical communities. Powder spreading is a critical step in SLM because it determines the density, flatness, and uniformity of the powder bed. However, defects such as pits, scratches, loose powder packing, nonuniform powder layer distribution, and particle segregation can occur during powder spreading. Further investigation is required because spreading metal-matrix diamond composite powders involves complex scientific and engineering challenges such as nonspherical particles and multicomponent powder systems. In this study, three blade-type spreader geometries (linear, circular, and parabolic) and a roller-type spreader are selected to investigate the effects of spreader structure on powder spreading quality and particle dynamics. The findings provide guidance for optimizing the powder spreading process in the SLM-based manufacturing of metal-matrix diamond tools.

Methods To achieve these objectives, diamond/CuSn powders were selected as the research materials, and three-dimensional geometries of the two types of powder particles were constructed. An adhesion force was incorporated into the particle contact model, which was based on the Hertz–Mindlin model and Johnson–Kendall–Roberts theory. A discrete element method (DEM) model was established to describe the microforces between the two types of powder particles. A DEM model of the powder spreading process was then developed, incorporating three blade-type spreader geometries (linear, circular, and parabolic) and a roller-type spreader. Parametric equations were used to modify the spreader geometries. The effects of spreader structural parameters on powder bed density and the uniformity of diamond distribution were investigated. Particle dynamics and the mechanisms of powder bed densification during spreading were analyzed. Furthermore, the physical mechanisms underlying particle segregation and jamming during powder spreading were elucidated.

Results and Discussions First, the effects of spreader geometry on powder bed quality were examined. When the structural coefficient angle θ of the linear blade increased from 0° to 90°, powder spreading quality changed only slightly. However, as θ increased from 90° to 150°, powder spreading quality improved significantly. Similarly, increasing the structural coefficient c of the circular blade from 0.25 to 1.25 mm significantly improved powder spreading quality. For the parabolic blade, increasing the structural coefficient p from 0.1 to 2.0 decreased the relative bulk density from 0.36 to 0.29 and increased the standard deviation from 0.031 to 0.041. Increasing the roller diameter also improved powder bed quality. Based on the optimized structural parameters considered in this study, the overall effects of the different spreader geometries on powder bed quality were comprehensively evaluated. The results indicated that the parabolic blade and roller spreaders provided relatively good powder spreading quality, followed by the circular blade, whereas the linear blade performed relatively poorly. Second, particle flow behavior was analyzed. With the translational motion of the spreader, the upper portion of the powder pile was sheared, pushing the particles forward. Particles in the lower portion of the pile passed through the gap between the spreader and the substrate, exhibiting flow behavior similar to that of particles passing through the orifice of a conical hopper. In addition, the roller induced complex particle diffusion and recirculating motion within the powder pile. Conversely, particle diffusion within the pile was relatively limited during blade-based spreading. The blade geometry had only a minor effect on particle trajectories. Diamond and CuSn particles exhibited similar overall flow patterns. Particles driven by the spreader moved horizontally and rose, fluctuated over a certain distance at higher positions, and then avalanched down the slope of the powder pile under gravity. Finally, particles passing through the gap between the spreader and the substrate were deposited onto the substrate. Next, particle contact force chains were examined. Increasing θ and c, whereas decreasing p, caused the blade to exert greater oblique downward pressure on the particles, increasing their nor-

mal contact forces and reducing the blade's shear effect on them. These changes enhanced powder bed quality. For the roller spreader, increasing the roller diameter increased the contact area between the roller and the powder pile, thereby increasing particle normal contact forces, enhancing compaction, and improving powder bed quality. Finally, the spatial distribution of the diamond particle volume fraction was analyzed. The spreader geometry had no significant effect on the overall variation in diamond particle volume fraction along the *X*-direction. However, the volume fraction first increased exponentially along this direction before fluctuating around the predetermined value. This pattern indicated particle segregation, with a relatively low diamond particle concentration near the front of the powder bed. The proposed mechanism was that the finer CuSn particles passed more readily through the gap between the spreader and the substrate and accumulated near the front of the powder bed. In contrast, the coarser, irregularly shaped diamond particles formed strong force chains, which contributed to particle jamming.

Conclusions Increasing the linear blade angle θ and the circular blade coefficient c, decreasing the parabolic blade coefficient p, and increasing the roller diameter d enhanced the oblique downward pressure exerted by the spreader on the particles, thereby increasing their normal contact forces and reducing the relative shear effect of the spreader. These changes improved powder bed quality. The results indicated that the parabolic blade and roller spreaders provided relatively good powder spreading quality, followed by the circular blade, whereas the linear blade performed relatively poorly. The diamond particle volume fraction initially increased exponentially along the *X*-direction and subsequently fluctuated around the predetermined value, indicating diamond particle segregation during powder spreading.

Key words: metal-matrix diamond; powder spreading processes; spreader structures; discrete element simulation; selective laser melting

（编辑　吴芝明）

引用格式: Huang Guoqin,Zhang Jiangtao,Zhu Xiaowei,et al.Effect of SLM spreader structures on the powder spreading dynamics mechanism of diamond tools[J].Advanced Engineering Sciences,2026,58(6):306–315.[黄国钦,张江涛,祝小威,等.SLM铺粉器结构对金刚石工具粉体铺展动力学机制的影响[J].工程科学与技术,2026,58(6):306–315.]